An incipient fault diagnosis methodology using local Mahalanobis distance: Fault isolation and fault severity estimation

Junjie Yang, Claude Delpha

▶ **To cite this version:**

Junjie Yang, Claude Delpha. An incipient fault diagnosis methodology using local Mahalanobis distance: Fault isolation and fault severity estimation. Signal Processing, 2022, pp.108657. 10.1016/j.sigpro.2022.108657 . hal-03696213

HAL Id: hal-03696213

https://centralesupelec.hal.science/hal-03696213

Submitted on 22 Jul 2024

HAL is a multi-disciplinary open access archive for the deposit and dissemination of scientific research documents, whether they are published or not. The documents may come from teaching and research institutions in France or abroad, or from public or private research centers.

L'archive ouverte pluridisciplinaire **HAL**, est destinée au dépôt et à la diffusion de documents scientifiques de niveau recherche, publiés ou non, émanant des établissements d'enseignement et de recherche français ou étrangers, des laboratoires publics ou privés.

Distributed under a Creative Commons Attribution - NonCommercial 4.0 International License

Version of Record: https://www.sciencedirect.com/science/article/pii/S0165168422001967
Manuscript_f50c7794bdc0f87c19933869b1b25419

An incipient fault diagnosis methodology using local Mahalanobis distance: Fault isolation and fault severity estimation

Junjie Yang, Claude Delpha*

Université Paris Saclay, CNRS, CentraleSupelec, Laboratoire des Signaux et Systemes (L2S), 3 Rue Joliot Curie, Gif sur Yvette, France

ARTICLE INFO

Keywords:
Incipient fault diagnosis
Faulty variable isolation
Fault severity estimation
Local Mahalanobis distance
Application to CSTR process

ABSTRACT

Recently, a detection methodology based on anchor estimation and the Mahalanobis distance, named the local Mahalanobis distance (LMD) technique, has been proposed for incipient fault detection. As an extension, this paper proposes the LMD based faulty variable isolation and fault severity estimation methods to offer an integrated incipient fault diagnosis solution. The LMD technique has been proved to be highly sensitive to incipient faults, robust to outliers, and free of distribution assumptions. Within the LMD framework, the faulty variable is recognized by analyzing the relative position of faulty samples and their corresponding anchors. Then an analytical expression of fault severity derived from the LMD index is established for the fault severity estimation task. Performance evaluations of the proposed methods based on a benchmark case of the Continuous-flow Stirred Tank Reactor (CSTR) process are provided in this work.The result shows that even for tiny deviation, such as 5dB fault to noise ratio, the total isolation performance still achieves 100% accuracy, and the relative error of two tricky faults in the case of severity estimation is less than 10%. The comparison study of different methods indicates that our solution outperforms divergence based techniques and reconstruction based contribution (RBC) methods for the two tasks.

Nomenclature

CSTR	Continuous-flow Stirred Tank Reactor
EPD	Empirical Probability Density
FNR	Fault to Noise Ratio
JSD	Jensen-Shannon Divergence
KLD	Kullback-Leibler Divergence
LMD	Local Mahalanobis Distance
LMDA	Local Mahalanobis Distance Analysis
MD	Mahalanobis Distance
MSE	Mean Squared Error
MSPM	Multivariate Statistical Process Monitoring
PCA	Principal Component Analysis
RBC	Reconstruction Based Contribution
SPE	Squared Prediction Error

1. Introduction

Fault diagnosis and prognosis are mandatory for modern complex systems surveillance due to the high requirements of reliability, availability, maintainability, and safety. Usually, a fault is conventionally defined as *"the unpermitted deviation of at least one process parameter from an acceptable condition"*, which can be distinguished according to their time dependencies, such as abrupt fault (stepwise), intermittent fault (pulsewise), and gradual fault [9, 15].

Figure 1 exhibits the evolution of three kinds of faults along with time. Abrupt fault suddenly appearing with a high amplitude may immediately cause system breakdown or severe performance degeneration. Intermittent fault appears randomly with a short time duration in the process, affecting system's performance for its repeated occurrence. In contrast to abrupt and intermittent faults, gradual fault does not affect system's performance dramatically at its early stage but, later, may result in severe system failures without taking any protective actions. Therefore, early diagnosis of gradual fault in their incipient stage is crucial to discover the potential risk of system breakdown, which is also becoming a hot topic in the fault diagnosis domain. Then incipient faults are defined as gradual ones with very low severities and possibly slowly varying evolution.

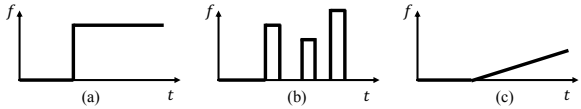

Figure 1: Three kinds of faults: a) abrupt fault; b) intermittent fault; c) gradual fault.

As pointed out in [26, 25, 39], incipient fault diagnosis is more challenging than other faults. Indeed, incipient fault creates tiny deviation that can easily be confused with noise or other disturbances, leading to the low effectiveness of conventional fault diagnosis methods. This work mainly involves the challenging problem of incipient fault diagnosis.

Generally, a fault diagnosis scheme includes three main tasks [9], fault detection, faulty sources isolation (sometimes

*Corresponding author
ORCID(s): 0000-0003-3224-8628 (C. Delpha)

© 2022 published by Elsevier. This manuscript is made available under the CC BY NC user license
https://creativecommons.org/licenses/by-nc/4.0/

treated as faults identification or classification), and fault severity assessment, as shown in Figure 2. They link to real applications like process state monitoring [6], anomaly detection [4], fault-tolerant control [37], remaining useful life estimation [28]. Fault detection is the first step in the fault diagnosis framework, aiming to recognize a faulty behavior with a short delay time. Then if a fault is detected, the isolation procedure proceeds to locate the key factors affecting the system's performance, which is usually realized based on some necessary assumptions, such as a defined fault type. Finally, the fault severity estimation module assesses how severe the fault is and helps to predict the fault evolution.

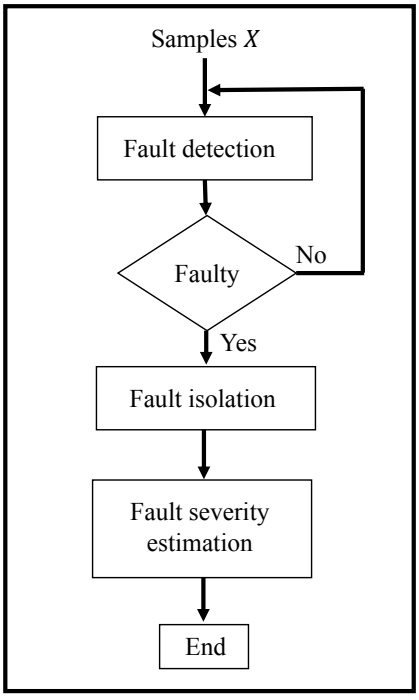

Figure 2: General incipient fault diagnosis framework

Fault detection is the foundation base for fault diagnosis and prognosis, naturally attracting huge attention in the literature and yielding various fault detection approaches. In particular, Multivariate Statistical Process Monitoring (MSPM) technique is one of the promising methodology branches. For example, it can be developed based on Principal Component Analysis (PCA), Independent Component Analysis (ICA), Fisher Discriminant Analysis (FDA), Partial Least Squares (PLS), Canonical Variate Analysis (CVA), Generalized Canonical Correlation Analysis (GCCA), etc. [20, 32, 23, 27, 7].

Commonly, the space partition idea is adopted in MSPM methods to obtain principal and residual subspace. Then, two statistics named Hotelling T^2 index and Squared Prediction Error (SPE) are often calculated based on the two subspaces, respectively, for fault detection purposes [32].

Further, additional statistic combining the T^2 and SPE indexes has been proposed, significantly improving the detection capability of MSPM methods [36]. Alternatively, several distance measures can be used in this area [3] and particular attention can be paid to the Mahalanobis distance [16]. The global Mahalanobis distance can be employed for fault detection problems with the benefit of avoiding the loss of information caused by space partition and dimension reduction [19].

Despite those improvements, to the best of our knowledge, the aforementioned approaches are still not sensitive enough to incipient faults [25, 29, 31]. Therefore, other types of MSPM approaches for incipient fault diagnosis have been proposed to improve the detection capability, such as Canonical Variate Dissimilarity Analysis (CVDA) [25] and Local Mahalanobis Distance Analysis (LMDA) [29, 31], where the latter is highly sensitive for incipient faults and effective for non-Gaussian distributed data. Alternatively, methodologies based on Kullback-Leibler Divergence (KLD) and Jensen-Shannon Divergence (JSD) are also effective for incipient fault detection [11, 33, 39].

Compared to the considerable progress of the fault detection problem using the previously mentioned techniques, the studies for incipient fault isolation and severity assessment are more tedious. Fault isolation problem aims at finding out the parameters or signals sources affected by a fault, and fault severity assessment is usually achieved by estimating the characteristics of the fault (amplitude, occurrence time, evolution function). Accurate solutions to both problems are necessary for fault tolerant control [17, 37], but also for the components' remaining useful life prediction [22] and the risk assessment of system breakdown [35] in industrial applications.

Concerning fault isolation and severity estimation problems, numerous model based methods specific to particular systems have been proposed, but they usually suffer from weak generalization capability for other systems. General methods for fault isolation and fault severity estimation problems are therefore attracting researchers' attention. Additionally, to take advantage of existing detection approaches' excellent characteristics, such as high sensitivity, reliability, and robustness, researchers tend to develop fault isolation and fault severity estimation methods based on the fault monitoring index.

For instance, KLD and JSD serve as fault detection indexes and subsequently are used for fault isolation and severity estimation [13, 10, 39]. The Reconstruction Based Contribution (RBC) technique is another promising branch developed on existing monitoring indexes for fault isolation and severity estimation, such as PCA based T^2 and SPE statistics [1], Mahalanobis Distance (MD), and Exponentially Weighted Moving Average (EWMA) [17, 18]. However, they are not sensitive enough to incipient faults especially when these low fault severities occur in extremely noisy environments. Besides, to the best of our knowledge, the discussion on the influence of fault severity relative to noise level is usually missing in previous works, but it is still crucial to evaluate the robustness performance of incipient fault diagnosis methods.

In order to cope with the major limitations of previous

works, this paper is dedicated to the development of new fault isolation and severity estimation approaches based on the LMD index, which has been proved to be highly sensitive to incipient faults. More specifically, we analyze the relative position of faulty samples compared to their reference anchors and calculate the contribution rate of each data variable being faulty. Subsequently, an analytical expression describing the relation between the fault amplitude and LMD index is developed for fault severity estimation. The benchmark case of the Continuous flow Stirred Tank Reactor (CSTR) process is used to verify and validate the performance of our proposal. Different fault severities relative to noise level are considered in the performance evaluation to show the performance bounds. Additionally, a comparative study with different approaches is performed to highlight the advantages of the proposed method.

Compared to the existed works related to fault diagnosis problems, the main contributions of this work are threefold.

1. Based on fault detection results, a new faulty variable isolation method indicating the fault contribution value of each faulty case is further proposed in this work. The proposed method is simple to implement and drastically improves isolation accuracy compared to existing approaches, especially for incipient faults.
2. The analytical expression connecting the fault severity and LMD index is established for fault severity estimation, which succeeds the advantages of LMD in the estimation procedure. So far, the LMD based incipient fault diagnosis framework, covering fault detection, fault isolation, and fault severity estimation, is completed.
3. The comprehensive performance evaluation, considering different fault severity relative to noise level and comparing different diagnosis approaches, is given in this work to reveal the different impacts of fault severity on methods' performance.

The remaining part of the paper is organized as follows. The relative works are reviewed in section 2. Section 3 revisits the LMD technique proposed for fault detection, including the definition of LMD and the anchors-generation algorithm. Then, the fault isolation method and the analytical expression for fault severity estimation are developed and derived in section 4. In section 5, the performance evaluation based on the CSTR process is carried out. Finally, the conclusion and discussion (section 6) close the paper.

2. Relative works

Several important works have made significant contributions to fault isolation and fault severity estimation problems [38, 5, 41, 14, 18], where divergence-based methods and reconstruction-based contribution techniques deserve particular attention for their high sensitivity or reliable performance. This section reviews the basic idea of these two groups of approaches and summarizes their advantages and limitations to provide an intuitive comparison with the method proposed in this work.

KLD combined with PCA feature extraction was first proposed for incipient fault detection [11, 33, 14]. It extracts data's principal components as features and uses KLD to assess features' divergences in probability distribution between healthy reference samples and testing samples. For that purpose, the features' probability density functions are estimated using the kernel density estimation approach. Afterwards, the theoretical model estimating the fault severity coefficient was then developed based on KLD using a known distributed assumption (Gaussian, Gamma) [12, 13, 10]. To isolate the single faulty variable, C. Delpha et al. further proposed the Z-decomposition to linearly combine variables with binary coefficient and calculated the KLD of the combined signals between reference and testing samples [10]. The detection result of all combined signals is decoded from binary code to determine a single faulty variable uniquely (e.g., the result 010 indicates that the third variable is faulty). Similar to KLD based approach, JSD was proposed with the same strategy to detect incipient faults, isolate faulty variables, and estimate fault severity, where the main benefit of using JSD is its higher sensitivity for incipient faults [39, 40].

Divergence-based methods are highly sensitive to incipient faults and robust to noise. However, they have at least two limitations. First, these approaches require a mass of samples to accurately estimate the probability density function. In addition, the theoretical model for fault severity estimation is only derived for Gaussian distributed data.

Another effective fault isolation and fault severity estimation approach is the reconstruction-based contribution (RBC) technique that combines the fault reconstruction idea and contribution plot technique [1, 18, 17]. To recover healthy signals from the faulty ones, RBC approaches reconstruct singles by removing the faulty component at a candidate fault direction. Subsequently, one of the monitoring indexes, such as Hotelling's T^2 statistics, SPE statistics [1], the combined statistics of T^2 and SPE [36], and Mahalanobis distance [8], is calculated to decide if the reconstructed signal is correctly recovered. Once the monitoring index of the reconstructed signal is lower than the detection threshold, the faulty direction indicating the faulty variables is determined, and the faulty component is obtained simultaneously.

RBC approaches have a solid theoretical foundation and can achieve a reliable fault diagnosis performance for severe fault severities with a distinct deviation from healthy conditions. However, the aforementioned monitoring indexes are not sensitive enough for tiny faults, leading to the low accuracy performance of the existing RBC approaches for incipient faults isolation and fault severity estimation. The goal of our proposal is then to cope with this limitation and then propose a robust and accurate solution for the incipient fault isolation and fault estimation problem.

3. LMD revisited

This section first reminds the LMD technique background to develop its basic concept. Then the LMD definition and its computational details are presented in the following sub-

sections, respectively.

3.1. Healthy region approximation

LMD originated from the healthy region approximation problem, which aims to specify an optimal healthy region based on fault-free data. The boundary of the healthy region is then used to distinguish between healthy and faulty samples. Due to the lack of fault's prior knowledge, it is tricky to obtain an accurate decision boundary. Moreover, outliers contained in fault-free data can also enlarge the healthy region. These two issues usually lead to the low sensitivity of typical methods for incipient fault diagnosis.

To cope with this issue, in our previous work [31], we proposed the LMD approach that can adaptively generate a healthy region for fault-free data. The adaptive healthy region consists of multiple overlapping sub-regions with different centers but the same radius, as shown in Figure 3 (a). In the training step, the centers of sub-regions, also referred to as anchors, are obtained by the anchors-generation algorithm, and the sub-region radius is selected as a threshold to guarantee a low false alarm rate. Even though the fault-free samples contain outliers, the generated healthy region is still accurate for unknown distribution.

When incipient faults occur, only a small part of samples deviates from the healthy condition, and its change is commonly tiny at its early stage, as shown in Figure 3 (b). In the fault detection procedure, an incipient faulty behavior can be detected if samples are out of the healthy region, which is easily realized by calculating the LMD index.

The theoretical analysis of LMD and its application to incipient fault for the early detection problem have been pioneered in our previous works [31, 29, 30]. In the following, we briefly revisit the LMD's definition and its training process basis for better understanding the fault isolation and fault severity estimation methods derived in the proposed work.

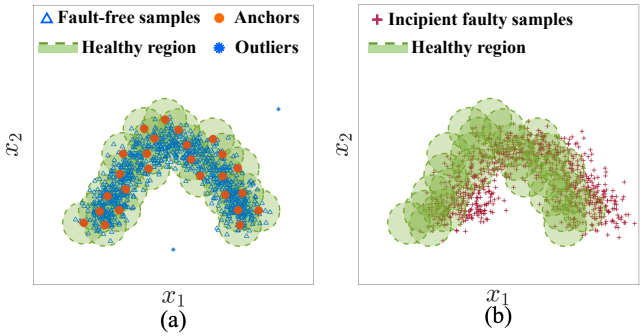

Figure 3: LMD operation example: (a) LMD training; (b) incipient fault detection

3.2. Local Mahalanobis distance

Considering two sample vectors $\boldsymbol{X}, \boldsymbol{Y}$ coming from the same distribution with mean vector $\boldsymbol{\mu}$ and covariance matrix $\boldsymbol{\Sigma}$, the multivariate Mahalanobis distance of a sample is calculated as:

$$d_M(\boldsymbol{X}) = \sqrt{(\boldsymbol{X}-\boldsymbol{\mu})^T\boldsymbol{\Sigma}^{-1}(\boldsymbol{X}-\boldsymbol{\mu})} \tag{1}$$

Then the Mahalanobis distance between two samples is easily derived as:

$$d_M(\boldsymbol{X},\boldsymbol{Y}) = \sqrt{(\boldsymbol{X}-\boldsymbol{Y})^T\boldsymbol{\Sigma}^{-1}(\boldsymbol{X}-\boldsymbol{Y})} \tag{2}$$

Based on the above definition, LMD is defined as the closest Mahalanobis distance from a sample to the healthy region. To enable the LMD calculation, the healthy region is approximated and represented as a finite number of points called anchors. If we denote the anchors set with κ elements as $S = \{\boldsymbol{C}_1, \cdots, \boldsymbol{C}_k, \cdots, \boldsymbol{C}_\kappa\}$, the LMD of a sample vector x is calculated as:

$$D(\mathrm{x}; S) = \min_k \{d_M(\mathrm{x}, \boldsymbol{C}_k) | \boldsymbol{C}_k \in S\} \tag{3}$$

Accordingly, sample's corresponding anchor, denoted as $\mathcal{A}(\mathrm{x})$, is derived as

$$\mathcal{A}(\mathrm{x}) = \arg\min_k \{d_M(\mathrm{x}, \boldsymbol{C}_k) | \boldsymbol{C}_k \in S\}, \tag{4}$$

Obviously, LMD is always a non-negative value for its distance property. Additionally, according to the definition, a larger LMD value usually implies a potential fault behavior since the observed sample is far from the healthy region. Therefore, based on this characteristic, LMD can be used to identify faulty samples, which has achieved promising incipient fault detection performance [31]. Besides the application for fault detection, LMD can be used to further characterize a fault, such as isolating the faulty variable and estimating the fault severity.

3.3. LMD training

In the LMD unsupervised training step, we aim to define a healthy region by determining its centers and a radius based on fault-free samples.

The first goal is achieved via the anchors-generation algorithm, whose basic idea is to extract critical spatial information by merging geometrically close fault-free samples as anchors [31]. Meanwhile, using the local density information of training samples, the algorithm identifies outliers and excludes them from generating anchors to obtain robustness ability against outliers [30]. Despite the similarity between the proposed anchors-generation algorithm and clustering methods to a certain extent, the proposed algorithm with its optimization procedure is necessary for LMD calculation to achieve optimal performance.

Here, we summarize the up-to-date anchors-generation procedure as Algorithm 1. For more details please refer to [30] and [31].

Given different parameters, this algorithm yields different anchors leading to diverse approximation performance. To achieve optimal performance, two parameters should be precisely tuned:

Algorithm 1 Anchor generating procedure

Require: Fault-free samples $\boldsymbol{X}^* = \{\mathrm{x}_i\}_{i=1}^K$, local radius γ, minimum number of local samples η
Ensure: Anchors set S

$\boldsymbol{\mu} \leftarrow \frac{\sum_{i=1}^K \boldsymbol{x}_i}{K}$
$\boldsymbol{C}_1 \leftarrow \boldsymbol{\mu}$
$\boldsymbol{\Sigma} \leftarrow \mathrm{cov}(\boldsymbol{X}^*, \boldsymbol{X}^*)$
$d_M(\mathrm{x}_i) \leftarrow \sqrt{(\mathrm{x}_i - \boldsymbol{\mu})\Sigma^{-1}(\mathrm{x}_i - \boldsymbol{\mu})^T}$
Rearrange fault-free samples as $\mathbb{Q}$ in ascending order according to $d_M(\mathrm{x}_i)$
$k \leftarrow 2$
repeat
  Take one sample x_i from $\mathbb{Q}$
  Find out $Z_k = \{\mathrm{x}_l | d_M(\mathrm{x}_i, \mathrm{x}_l) < \gamma, l > i, \mathrm{x}_l \in \mathbb{Q}\}$
  $n_k \leftarrow$ samples number in Z_k
  if $n_k < \eta$ **then** Continue
  end if
  $\boldsymbol{C}_k \leftarrow \frac{1}{n_k} \sum_{q=1}^{n_k} \mathrm{x}_q (\mathrm{x}_q \in Z_k)$
  Remove Z_k from $\mathbb{Q}$
  $k \leftarrow k + 1$
until $\mathbb{Q}$ is empty
$S \leftarrow \{\boldsymbol{C}_1, \cdots, \boldsymbol{C}_k, \cdots, \}$
return S;

- On the one hand, η indicating the minimum allowed samples number is designed to identify potential outliers, which should be firstly tuned according to outliers' number. The experiment results given in [30] indicates that $\eta = 2$ is the usual setting for outliers' number less than 10%, otherwise a larger η should be considered when data contain lots of outliers.

- On the other hand, the local radius γ specifies the size of a local region for sample merging, which affects the approximation accuracy. A large local radius usually leads to a small anchors' number and a rough description of the healthy domain. Conversely, a small local radius increases the accuracy but may cause an overfitting problem.

  To explicitly analyze this factor, the approximation error related to γ value is quantified as:

$$\mathrm{Err} = \sum_{i=1}^{K} D(\mathrm{x}_i; S), \quad (\mathrm{x}_i \in \boldsymbol{X}^*) \tag{5}$$

  The example shown in Figure 4 indicates that the error revolution against the local radius is always convex regardless of η value. The optimization procedure then can be implemented by searching the corresponding γ^{opt} that minimizes Eq.(5).

The second part of LMD training is to select the healthy local radius, also called healthy region margin. To that end, the distribution model of the LMD index in the null case is established by using the generalized extreme value distribution model. For the given significance level, the margin is then determined based on this estimated probability model. Since this part is only relative to fault detection, no more additional details of margin selection will be presented here, but they are accessible from [31].

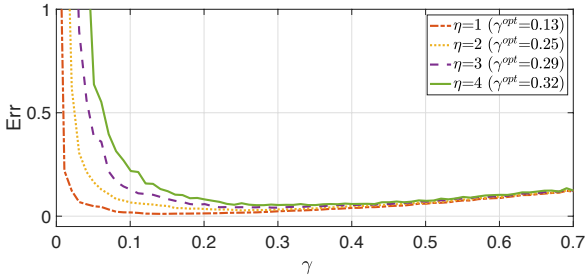

Figure 4: Evolution of approximation error for different γ and η

In the following, for the proposed incipient fault diagnosis procedure, the optimal anchors set is computed and directly used for LMD calculation.

4. Fault isolation and estimation procedure

Let's assume that a fault was detected by using the LMD-based detection method. Subsequently, in this section, we propose the LMD-based fault isolation method to identify the faulty source, and then assess its fault severity degree by estimating the amplitude of the faulty component. In contrast to the fault detection process, fault's prior knowledge is required in these two diagnosis procedures. Therefore, a fault model and the necessary assumptions are first given.

4.1. Assumptions and fault modeling

In this work, we do not make any assumptions about data distribution since the LMD technique can adapt to unknown distributions. However, the following assumptions are required for developing the proposed fault isolation and estimation methods.

- Assumption 1: The fault type is confined to additive fault with incipient nature for simplifying the fault's behavior. The additive form indicates that any faulty signal can be split up into a healthy part and a faulty component, which is a conventional way to describe the fault's influence on data.

- Assumption 2: This work only considers the single faulty source situation. This assumption is reasonable because single faults are more common, and our isolation method can be easily generalized to multiply cases without additional modification.

Based on these assumptions, we develop a fault model for the subsequent fault diagnosis methods. Let us consider a faulty dataset $\boldsymbol{X} = (\boldsymbol{x}_1, \cdots, \boldsymbol{x}_j, \cdots, \boldsymbol{x}_m)$ with m variables and N observations, where the observation of $\boldsymbol{x}_j$ is denoted as $\mathrm{x}_j = [x_{1j}, \cdots, x_{ij}, \cdots, x_{Nj}]^T$. Then let a fault occurs from the bth observations at the cth variable. In other words, the

last $N-b+1$ observation of the cth variable are faulty. According to [11], a faulty signal $\boldsymbol{x}_c$ with an additive fault can be decomposed into fault-free signal $\boldsymbol{x}_c^*$ and faulty component $\boldsymbol{f}$, such as:

$$\boldsymbol{x}_c = \boldsymbol{x}_c^* + \boldsymbol{f} \tag{6}$$

For the given fault occurrence position b, the faulty component can be written as:

$$\boldsymbol{f} = [0, \cdots, 0, f_b, \cdots, f_N]^T \tag{7}$$

Further, we use the first-order model to describe the evolution of incipient faults, such as

$$f_i = \delta \cdot (i-b+1) \cdot T_e, \quad (i \geq b) \tag{8}$$

where δ is the fault severity that can be seen as a constant in small duration, and T_e is the sampling time.

For incipient fault diagnosis, the discussion of fault severity without considering noise is meaningless. Therefore, the fault-to-noise ratio (FNR) is considered and widely used in the incipient fault diagnosis topic. It is defined as:

$$\text{FNR} = 10 \log \frac{p_f}{p_n} \tag{9}$$

where p_n is the noise power, and p_f is the power of faulty component.

Based on the fault model derived in Eq.(8), the fault power p_f can be developed as:

$$\begin{aligned} p_f &= \frac{\sum_{i=b}^{N} f_i^2}{N} = \frac{\sum_{i=1}^{N-b+1} \delta^2 i^2 T_e^2}{N} \\ &= \frac{\delta^2 T_e^2 (N-b+1)(N-b+2)(2N-2b+3)}{6N} \end{aligned} \tag{10}$$

Using this Eq.(10), the FNR can be derived and the influence of the fault severity for a given noisy environment can be studied.

Note that generally, the samples' number N is widely large, and $N-b$ is a sufficient number of faulty samples. For the isolation and estimation procedures, only these faulty samples are considered. A low number of faulty samples will reduce the fault power and increase the difficulty of diagnosis, particularly in noisy environments.

4.2. Faulty variable isolation method

In the LMD based fault detection scheme, the corresponding anchor of a sample is first located, serving as a reference position for fault analysis. When a fault occurs, the faulty samples dramatically deviate from their references, while healthy samples are close to the corresponding anchors. These two cases can be distinguished by calculating the Mahalanobis distance between samples and anchors (LMD). In few words, the distance information is used for the fault detection task.

Similarly, we consider the change of samples' relative position for the fault isolation task. The position's change is based on observed samples and their corresponding anchors, where the latter has been obtained in the previous detection step. Given a samples vector x_i and its corresponding anchors vector $\mathcal{A}(\mathrm{x}_i)$, the position's change with normalization weight is presented as:

$$\boldsymbol{G}_i = (\mathrm{x}_i - \mathcal{A}(\mathrm{x}_i))^T \mathcal{W} \tag{11}$$

where $\mathcal{W}$ is the diagonal matrix consisting of the standard deviation σ_j of each healthy variable, such that:

$$\mathcal{W} = diag\{\sigma_1^{-1}, \cdots, \sigma_m^{-1}\} \tag{12}$$

The weight is used here to unify the scale of different variables.

As illustrated in Figure 5, we use a toy example with two variables to show how the position's change information contributes to faulty source isolation. In fact, when a variable is affected by a fault, faulty samples will deviate in a certain direction. In this example, the first variable x_1 is affected, and thus the first element of the sample vector increases from x_1^* to $(x_1^* + F)$. We show the faulty sample and its healthy version to highlight this change. However, the increment F in x_1 direction is invisible for the unknown healthy version until introducing a reference point, the anchor. For healthy cases, since samples are close to their anchors, the deviation of samples with respect to their anchors in different directions is small. In contrast, faulty samples are far away from their anchors. With the single fault assumption, there is always a distinct shift of faulty samples in one direction. In other words, the single faulty variable can effectively be isolated by observing the increment of faulty samples in different directions, which is reflected by the change vector $\boldsymbol{G}$.

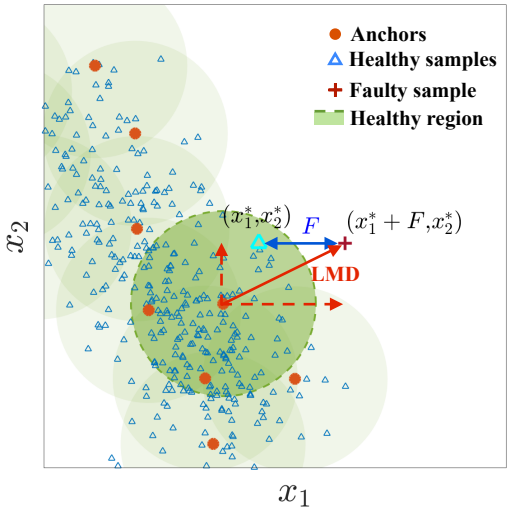

Figure 5: Two-dimensional example for LMD based fault isolation

Regarding the incipient faults, the reliability of sample based results $\boldsymbol{G}_i$ is easily impacted by noise, especially at its

early stage. Therefore, a number of sequential faulty samples are used for the final decision to increase the reliability and isolation accuracy. Suppose a fault is detected at the b'th observation, and then the average position change vector can be calculated as:

$$\bar{\boldsymbol{G}} = \sum_{i=b'}^{N} \boldsymbol{G}_i \tag{13}$$

Let $\bar{\boldsymbol{G}} = [g_1, \cdots, g_j, \cdots, g_m]$. The Softmax function is further applied to elements of $\bar{\boldsymbol{G}}$ for the unifying purpose. Then the fault contribution $\boldsymbol{P}_j$ of each variable is calculated as:

$$\boldsymbol{P}_j = \frac{e^{|g_j|}}{\sum_{k=1}^{m} e^{|g_k|}}, \quad 0 \le \boldsymbol{P}_j \le 1 \tag{14}$$

Finally, for a single faulty variable case, the faulty variable index number is recognized as:

$$\hat{c} = \arg\max_j \boldsymbol{P}_j \tag{15}$$

The corresponding $\boldsymbol{x}_{\hat{c}}$ faulty variable is then isolated.

Remarkably, even though the proposed isolation method is dedicated to the single faulty source situation, its generalization to multiple fault cases is possible. The most distinct faulty source can be isolated first by using this method. Then we can reduce the isolated faulty signal from the data, and reuse the proposed isolation method to identify the second faulty source. This work will not further analyze the isolating performance of the proposed method for multiple faults cases.

4.3. Fault severity estimation method

Once the faulty variable is isolated, the fault severity estimation procedure is activated. This latter is dedicated to the estimation of the coefficient δ of the first-order approximation written in Eq.(8) by explicitly establishing its expression based on the LMD index.

Similarly to Eq.(6), a faulty sample vector x_i also can be decomposed as:

$$\mathrm{x}_i = \mathrm{x}_i^* + f_i, \quad (i \ge b) \tag{16}$$

Substituting Eq.(4) and Eq.(16) into Eq.(3), we can develop LMD as

$$\begin{aligned} D(\mathrm{x}_i, S) &= d_M(\mathrm{x}_i, \mathcal{A}(\mathrm{x}_i)) \\ &= \sqrt{[\mathrm{x}_i - \mathcal{A}(\mathrm{x}_i)]^T \Sigma^{-1} [\mathrm{x}_i - \mathcal{A}(\mathrm{x}_i)]} \\ &= \| \, [\mathrm{x}_i - \mathcal{A}(\mathrm{x}_i)]^T \Sigma^{-\frac{1}{2}} \, \|_2 \\ &= \| \, [\mathrm{x}_i^* + f_i - \mathcal{A}(\mathrm{x}_i)]^T \Sigma^{-\frac{1}{2}} \, \|_2 \end{aligned} \tag{17}$$

where $\| \cdot \|_2$ corresponds to the L^2 norm.

For simplicity, we define the following three notations:

$$\boldsymbol{\zeta}_i = \mathrm{x}_i^* - \mathcal{A}(\mathrm{x}_i) \tag{18}$$

$$\boldsymbol{\zeta}_i' = \boldsymbol{\zeta}_i \Sigma^{-\frac{1}{2}} = [\zeta_{i1}', \cdots, \zeta_{ij}', \cdots, \zeta_{im}'] \tag{19}$$

$$\Sigma^{-\frac{1}{2}} = \begin{bmatrix} \varsigma_{11} & \cdots & \varsigma_{1j} & \cdots & \varsigma_{1m} \\ \vdots & & \vdots & & \vdots \\ \varsigma_{j1} & \cdots & \varsigma_{jj} & \cdots & \varsigma_{jm} \\ \vdots & & \vdots & & \vdots \\ \varsigma_{m1} & \cdots & \varsigma_{mj} & \cdots & \varsigma_{mm} \end{bmatrix} \tag{20}$$

With the above notations and first-order approximation model Eq.(8), we further develop Eq.(17) to Eq.(21).

Although Eq.(21) establishes the link between δ and LMD index, δ can not be calculated directly through this equation for the unknown ζ_{ij}'. However, Eq.(21) is the quadratic function of sample index i, which can be simplified as:

$$D^2(\mathrm{x}_i; S) = a_2 i^2 + a_1 i + a_0 \tag{22}$$

where

$$a_2 = \delta^2 T_e^2 \sum_{j=1}^{m} \varsigma_{cj}^2 \tag{23}$$

$$a_1 = 2\delta T_e \sum_{j=1}^{m} \zeta_{ij}' \varsigma_{cj} + 2(1-b)\delta^2 T_e^2 \sum_{j=1}^{m} \varsigma_{cj}^2 \tag{24}$$

$$a_0 = 2(1-b)\delta T_e \sum_{j=1}^{m} (\varsigma_{cj}^2 + \zeta_{ij} \varsigma_{cj}) + \| \, \zeta_i' \, \|_2^2 \tag{25}$$

In fact, $D^2(\mathrm{x}_i; S)$ has been calculated for fault detection, and i is known. Therefore, the coefficients a_0, a_1, a_2 can be easily estimated by the polynomial curves fitting technique. More accurately, the solution for Eq.(22) is obtained by minimizing the sum of squared errors between the true and estimated D^2 values based on samples from b' to N.

In order to derive the calculation process, we let:

$$W = [a_0, a_1, a_2] \tag{26}$$

$$\Xi^T = \begin{bmatrix} 1 & \cdots & 1 & \cdots & 1 \\ b' & \cdots & i & \cdots & N \\ b'^2 & \cdots & i^2 & \cdots & N^2 \end{bmatrix} \tag{27}$$

and

$$Y = [D^2(\mathrm{x}_{b'}; S), \cdots, D^2(\mathrm{x}_i; S), \cdots, D^2(\mathrm{x}_N; S)]^T \tag{28}$$

The coefficients vector W can be calculated as:

$$W = (\Xi^T \Xi)^{-1} \Xi^T Y \tag{29}$$

Finally, the fault severity δ is estimated as $\hat{\delta}$ as follows:

$$\hat{\delta} = \sqrt{\frac{a_2}{T_e^2 \sum_{j=1}^{m} \varsigma_{cj}^2}} \tag{30}$$

Based on this theoretical study, the efficiency of the estimation can be evaluated.

$$
\begin{aligned}
D^2(\mathrm{x}_i; S) &= \| \zeta_i' \|_2^2 + 2 f_i \sum_{j=1}^{m} \zeta_{ij}' \varsigma_{cj} + f_i^2 \sum_{j=1}^{m} \varsigma_{cj}^2 \\
&= \| \zeta_i' \|_2^2 + 2\delta (i-b+1) T_e \sum_{j=1}^{m} \zeta_{ij}' \varsigma_{cj} + \left[\delta (i-b+1) T_e\right]^2 \sum_{j=1}^{m} \varsigma_{cj}^2 \\
&= i^2 \left(\delta^2 T_e^2 \sum_{j=1}^{m} \varsigma_{cj}^2 \right) + 2i \left[\delta T_e \sum_{j=1}^{m} \zeta_{ij}' \varsigma_{cj} + (1-b) \delta^2 T_e^2 \sum_{j=1}^{m} \varsigma_{cj}^2 \right] + 2(1-b) \delta T_e \sum_{j=1}^{m} \left(\varsigma_{cj}^2 + \zeta_{ij} \varsigma_{cj} \right) + \| \zeta_i' \|_2^2
\end{aligned} \tag{21}
$$

5. Performance analysis

In this section, the CSTR process is used as a case study to validate the effectiveness of the faulty variable isolation method and evaluate the performance of the fault severity estimation model. Note that the proposed methods are not limited to one specified system but can be applied to other complex systems [21] and sensor network [2].

5.1. CSTR process

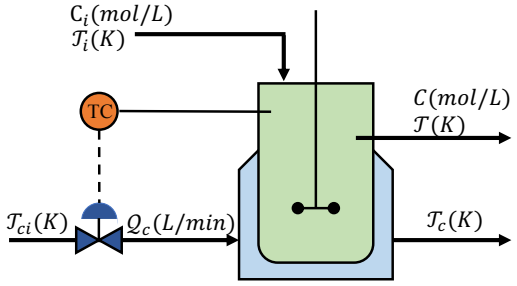

Figure 6: Schematic diagram of the CSTR process

As a benchmark case, the CSTR process is frequently used to evaluate fault diagnosis methodologies [34, 30, 24]. The schematic diagram of the CSTR process is displayed in Figure.6, where an exothermic reaction takes place in a reactor surrounded by a jacketed tank. In the process, a fluid stream is fed to the reactor and perfectly mixed with catalysts. The reactor temperature is maintained by feeding a coolant medium at a lower temperature. The model can be described as following exothermic first-order reactions,

$$
\frac{dC}{dt} = \frac{Q}{V}(C_i - C) - \beta C q_0 e^{\left(\frac{-E}{RT}\right)} + \nu_1 \tag{31}
$$

$$
\frac{d\mathcal{T}}{dt} = \frac{Q}{V}(\mathcal{T}_i - \mathcal{T}) - \beta \frac{\Delta H_r q C}{\varphi C_p} - h \frac{\mathcal{U}\mathrm{A}}{\varphi C_p V}(\mathcal{T} - \mathcal{T}_c) + \nu_2 E \tag{32}
$$

$$
\frac{d\mathcal{T}_c}{dt} = \frac{Q_c}{V_c}(\mathcal{T}_{ci} - \mathcal{T}_c) + h \frac{\mathcal{U}\mathrm{A}}{\varphi_c C_{pc} V_c}(\mathcal{T} - \mathcal{T}_c) + \nu_3 \tag{33}
$$

where the outputs of the process are the reactor temperature ($\mathcal{T}$), the concentration in the reactor (C), the coolant temperature ($\mathcal{T}_c$), and the coolant flow rate ($\mathcal{Q}_c$). The system's inputs are the input flow concentration (C_i), the flow temperature ($\mathcal{T}_i$), and the coolant flow temperature ($\mathcal{T}_{ci}$). Notations of the above equations are given in Table 1.

Table 1
Notations for CSTR Process

Parameter	Description
$\mathcal{T}$	Reactor temperature
$\mathcal{T}_c$	Coolant temperature
$\mathcal{T}_i$	Flow temperature
$\mathcal{T}_{ci}i$	Coolant flow temperature
C	Concentration in the reactor
C_i	Input flow concentration
$\mathcal{Q}_c$	Coolant flow rate
$\mathcal{Q}$	Inlet flow rate
V	Tank volume
$\mathcal{U}$A	Heat transfer coefficient
V_c	Jacket volume
q_0	Pre-exponential factor
ΔH_r	Heat of reaction
φ, φ_c	Fluid density
E/R	Activation energy
C_p,C_{pc}	Fluid heat capacity
$\nu_{1,2,3}$	Process noise

The corresponding simulation model introduced by Karl Ezra Pilario in [24] is one of the most influential models for its easy access and professional design. It can simulate the healthy case and ten different faulty scenarios as defined in Table 2. Fault 1 and 2 simulate catalyst decay and heat transfer fouling. Fault 3 simulates these two faults' simultaneous evolution, and Fault 4 to 10 correspond to additive faults simulating sensor drifts. Therefore, to satisfy assumption 1, we only consider Fault 4 to 10 in this validation procedure and relabeled them as F_1 to F_7, respectively. Note that the subscript of F indicates the single faulty variable (assumption 2).

In the validation procedure, the following settings of the simulation and methods should be noticed:

- The system's input $\boldsymbol{u} = [C_i \ \mathcal{T}_i \ \mathcal{T}_{ci}]$ and the output $\boldsymbol{y} = [C \ \mathcal{T} \ \mathcal{T}_c \ \mathcal{Q}_c]$ were concatenated to form the process data $\boldsymbol{X} = [\boldsymbol{u}, \boldsymbol{y}]$.
- For data generation, the signals were sampled every minute for a total duration of 20 hours. In other words, the sampling time $T_e = 1$ (min) and the samples' number $N = 1200$.

Table 2
Description of the faulty scenarios

ID	Fault	Description	Type
-	1	$\beta = \beta_0 e^{-\delta t}$	Multiplicative
-	2	$h = h_0 e^{-\delta t}$	Multiplicative
-	3	fault 1 and 2	Multiplicative
F_1	4	$C_i = C_{i,0} + \delta t$	Additive
F_2	5	$\mathcal{T}_i = \mathcal{T}_{i,0} + \delta t$	Additive
F_3	6	$\mathcal{T}_{ci} = \mathcal{T}_{ci,0} + \delta t$	Additive
F_4	7	$C = C_0 + \delta t$	Additive
F_5	8	$\mathcal{T} = \mathcal{T}_0 + \delta t$	Additive
F_6	9	$\mathcal{T}_c = \mathcal{T}_{c,0} + \delta t$	Additive
F_7	10	$\mathcal{Q}_c = \mathcal{Q}_{c,0} + \delta t$	Additive

- In the training process, 10 groups of fault-free data with 1200 samples for each were used to construct the fault-free data matrix $\boldsymbol{X}^*$.
- The anchors-generation algorithm was applied on $\boldsymbol{X}^*$ with $\eta = 2$. The optimization procedure is then activated, yielding the optimal local radius $\gamma^{opt} = 1.448$ and 224 anchors.

  The parameters were properly tuned to reach a satisfactory detection performance, and then continue to be used in this experiment for isolation and fault estimation.
- In the fault diagnosis procedures, the system regenerates all the input and output signals with varying operation conditions and random noise. A fault was introduced at 1000 minutes for all faulty scenarios, so that $b = 1001$.
- The fault is assumed to be detected correctly without time delay in the experiment, i.e., $b' = b$, and the prior knowledge of the true faulty variable is used for fault estimation. This setting is not necessary for practice but allows the independent discussion of performance for each diagnosis procedure because their effectiveness highly depends on their previous step. Note that this setting is the same for all compared methods.

5.2. Fault isolation validation results

Firstly, to validate the proposed faulty variable isolation method, we generated 1 healthy and 7 faulty cases (F_1 to F_7) data with SNR=30dB and FNR=20dB. According to Eq.14 derived in section 4.2, the fault contribution of each variable for different cases was calculated and shown in Figure 7. The results are divided into 8 groups, the healthy one and 7 faulty ones named as F_1 to F_7. For each group, the first bar stands for the fault contribution of the first variable, and so on. In the healthy group, all contribution values are close and lower than 0.15. This means that all the variables contribute quite similarly to the healthy case. For the faulty groups, the contribution calculation highlights one variable with a larger contribution value than others: it corresponds to the true faulty variable that has been identified.

For example, in the group F_1 whose true faulty variable is the first one, the contribution of the first variable has the largest value 0.22. Therefore, the faulty variable of F_1 faulty case can be correctly determined by applying the proposed fault isolation method based on Eq.15.

To evaluate the method's reliability and discrimination ability among different faulty variables, we repeated the fault isolation experiment 1000 times for each faulty case and calculated the confusion matrix, which is shown in Figure 8. The result demonstrates that our isolation method achieves 100% accuracy for all faulty cases under 20dB FNR condition. This means that if the noise power is not so close to the fault severity we can accurately perform the fault isolation with excellent reliability.

Despite the above promising isolation result, observing the contribution values of all faulty cases, we notice that the results of F_4 and F_7 seem less significant than others, which implies that these two cases are the most challenging for isolation procedure. Therefore, to study the impact of fault severity on the isolation procedure, the accuracy performance was further evaluated for FNR=0dB.

Figure 9 exhibits the confusion matrix under this condition, showing that the accuracy of F_4 and F_7 cases significantly decreases. The case F_4 is confused with F_1 in 12.5% of realizations and confused with F_3 in 7.1% of realizations. Although, the accuracy for F_7 case is slightly better than F_4, there are 5.1% of confusing results with F_3. Besides, the accuracy for F_1 and F_5 also slightly decrease (at least 99.8% of accuracy), but they are still at a very high level. Our isolation procedure can then be considered as accurate enough for identifying correctly the faulty features.

The falling accuracy for decreasing FNR indicates that the real challenge for incipient fault diagnosis lies in the tiny fault with power close to or lower than noise power. To intensely discuss this challenge, we considered different FNR conditions and compared our method with existing isolation approaches, including two divergence based methods (KLD and JSD) and two RBC methods based on MD and the combined statistical tests T^2 and SPE.

Figure 10 displays the total accuracy of 5 methods for the 7 considered faulty cases along with varying FNR values. The result shows that the proposed method mentioned as LMD in the figure outperforms others. For FNR> 3dB, the LMD based proposed method can achieve 100% of accuracy. Only the MD based RBC method can have close results. The three other types of techniques are not accurate enough. Although the accuracy of the LMD based method starts to decrease when FNR< 3dB, its high accuracy performance is satisfying for FNR larger than −5dB. It can be noticed that the MD based RBC method has the same high accuracy as the LMD based method when FNR> 8dB, while its performance significantly decline if tiny fault severities are considered like for FNR< 5dB. According to these comparison results, the other three mentioned approaches are all ineffective for fault isolation of the CSTR process.

The results displayed in Figure 10 also indicate that the FNR range from 2dB to 8dB is critical for fault amplitude's

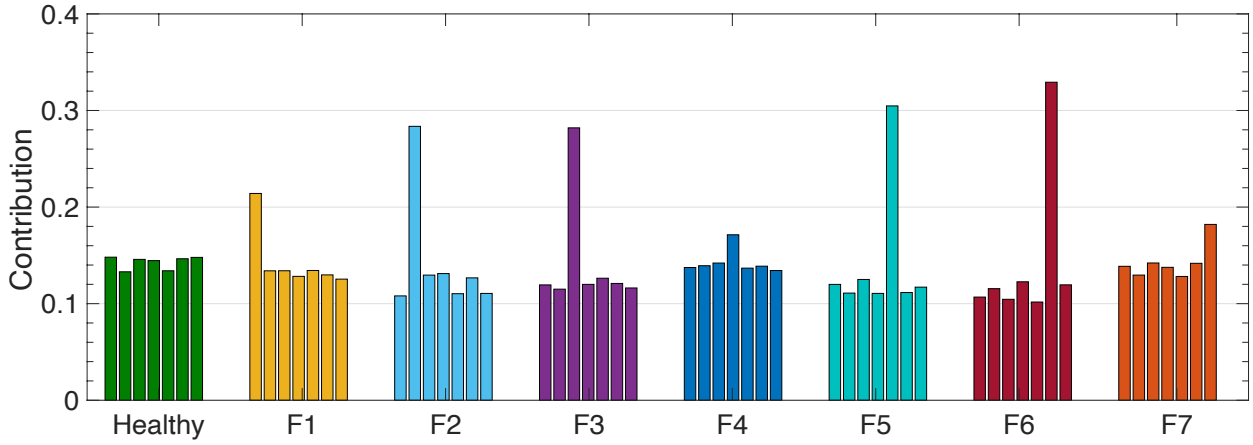

Figure 7: Contribution result of each variable for 1 healthy and 7 faulty cases

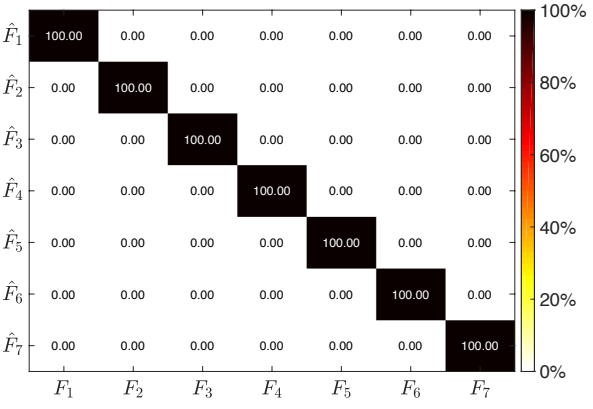

Figure 8: Confusion matrix of the proposed method for FNR=20dB

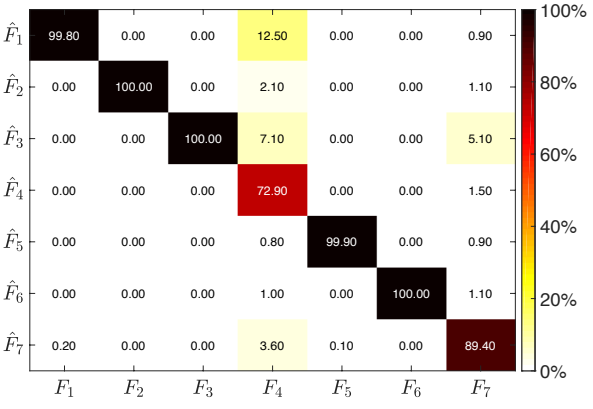

Figure 9: Confusion matrix of the proposed method for FNR=0dB

change identification. Below 2dB, the fault's symptom is too tricky to be diagnosed properly: the fault power is very close to the noise power. Above 8dB, the difference between these two powers is sufficient to make the fault recognizable. In this critical range, the accuracy performances of the

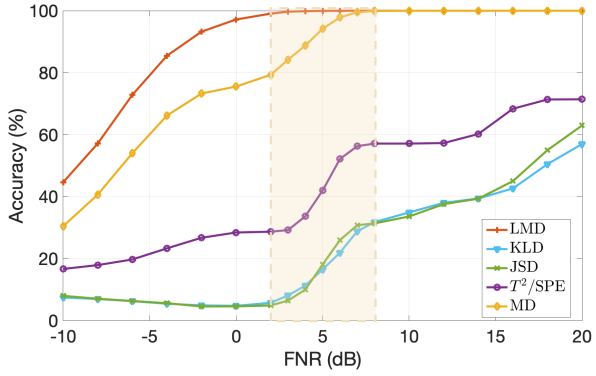

Figure 10: Total isolation accuracy performance of different methods along with varying FNR values

five methods are all degraded with FNR decreasing, where the T^2/SPE, KLD-based, and JSD-based methods have the most conspicuous performance degeneration (about 30%). Although both the LMD-based and MD-based methods have good performance in large FNR conditions, the performance of the MD-based method is reduced by 20% in this critical range, and the LMD-based method is almost unchanged. The significant performance difference in the critical range shows that the proposed method is more sensitive to incipient faults than other approaches.

To appreciate the limitation of those five methods, the obtained accuracy results of each faulty case for FNR=0dB are also displayed in Figure 11.

Consistent with the result of Figure 9, F_4 and F_7 are the two most difficult cases to isolate for all methods. In other words, the main limitation of these methods lies in the relatively weak isolation ability for F_4 and F_7 cases. For example, the worse total performance of the MD based RBC method compared to the LMD-based method is mainly caused by its low accuracy performance for the two challenging cases. Conversely, although the total performance of T^2/SPE method is poor, its accuracy for F_3 case remains promising.

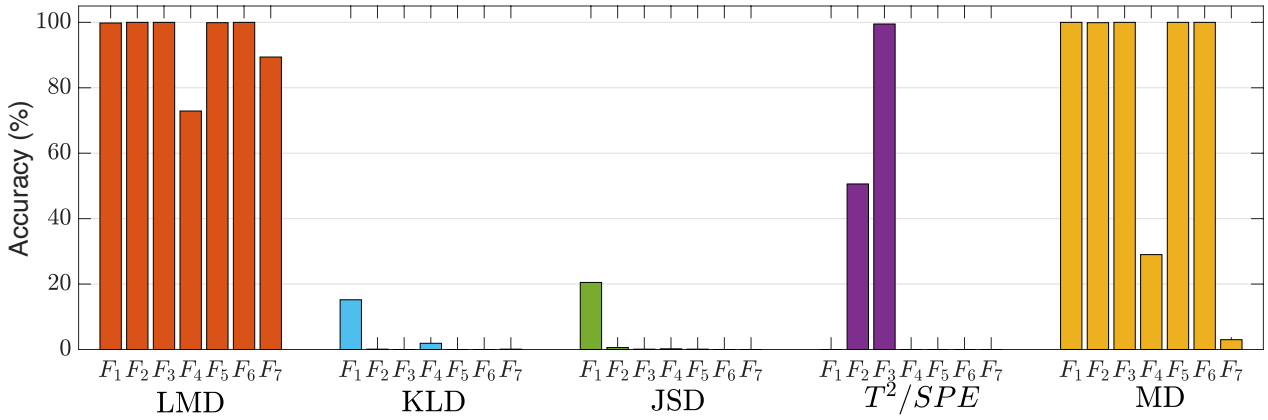

Figure 11: Accuracy of different methods for each faulty case with FNR=0dB

5.3. Fault estimation validation results

After the isolation of the faulty variable, the fault severity estimation procedure, as derived in section 4.3, can start based on the fault detection and isolation results obtained from the previous steps.

Firstly, as an example, we show in Figure 12 the LMD result of the faulty case F_4 with SNR=30dB (given noise) and FNR=20dB (given fault severity). In this figure, the fault occurs at 1000 min as marked by the dotted box. The increasing trend of the LMD results not only indicates the occurrence of a fault but also contains its evolution information.

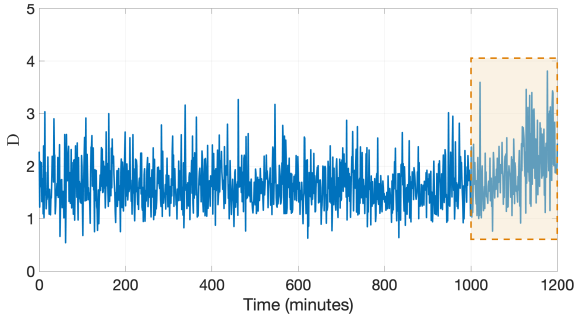

Figure 12: Example of LMD result with SNR=30dB and FNR=20dB. The fault occurs at 1000 min and affects 4^{th} variable

Based on the fault growing tendency, our method is applied to estimate the value of δ using the derived Eq.30 in section 4.3. Figure 13 demonstrates the different true values of δ versus its estimated ones for F_4 case. Basically, with δ value increasing from 4×10^{-4}, the evolution of $\hat{\delta}$ shows asymptomatic consistency of true fault severity values. However, with δ decreasing to an extremely small value, such as $\delta < 4 \times 10^{-4}$, the result highlights an opposite evolution tendency. Moreover, this tendency develops to reach an overestimated behavior for tiny fault severities.

To unify the estimation error of the different studied faulty

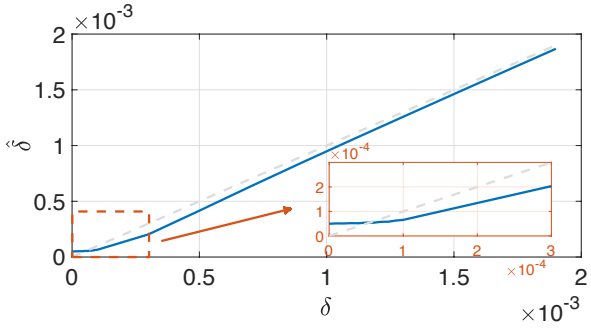

Figure 13: Estimated result $\hat{\delta}$ versus the true value δ

cases, the relative error is used such as:

$$\epsilon(\%) = \frac{\hat{f} - f}{f} \times 100 = \frac{\hat{\delta} - \delta}{\delta} \times 100 \tag{34}$$

Figure 14 shows relative errors for all faulty cases with SNR=30dB and varying FNR from -10dB to 20dB. It can be noticed that all faulty cases have similar evolution tendencies: with fault severity decreasing (FNR decreasing), the relative error decrease from a negative value (underestimation) and then increase to be positive (overestimation). Remarkably, consistent with fault isolation, F_4 and F_7 are also the two most challenging cases for fault severity estimation: they have the worst estimation performance than the other faulty cases.

Accordingly, in order to deeply discuss the estimation performance for these two challenging cases, we calculated another typical error criterion, the mean square error (MSE), and compared the result of the proposed method with that of the previously mentioned methods. Figure 15 displays the MSE results in the case of F_4 for all the considered techniques. It highlights that the LMD based method always achieves the minimal error for all FNR conditions. Although the MD based method has pronounced isolation performance, its fault severity estimation capability is significantly weaker than divergence based methods and the LMD one. The two

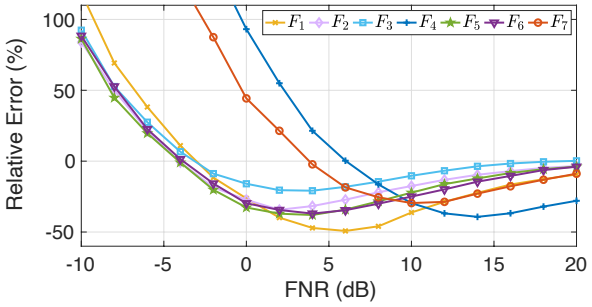

Figure 14: Relative errors of the proposed method for the 7 faulty cases

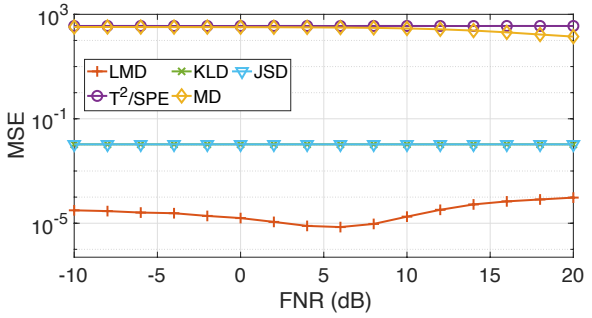

Figure 15: Mean squared error for different methods in the case of F_4

divergence based methods (KLD and JSD) have almost the same considerable estimation accuracy, but we can remind that they are not suitable for fault isolation. The poor performance of T^2/SPE based RBC method for both fault isolation and severity estimation indicates that it is ineffective for incipient fault diagnosis.

The estimation error for case F_7 exhibited in Figure 16 shows a similar result as F_4. The LMD proposed method

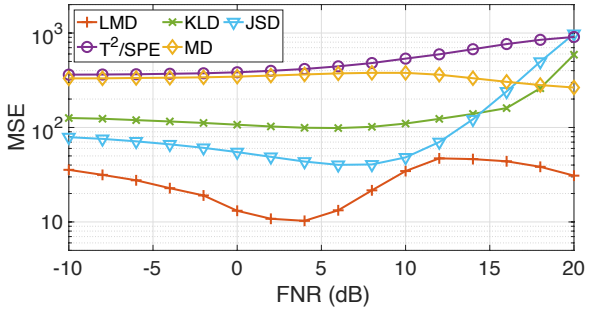

Figure 16: Mean squared error for different methods in the case of F_7

achieves the best performance. The two divergence based methods are slightly worse than LMD's, and the two RBC based methods are unreliable. Additionally one can note that, for this faulty case, the JSD method offers a lower error than KLD for small fault severity with that noise level, which actually verifies its higher sensitivity for fault severity estimation in these noisy environments.

6. Conclusion

In this paper, we propose faulty variable isolation and fault severity estimation methods based on the LMD index and its anchors generation algorithm, which, together with the LMD based fault detection method, completes the LMD based incipient fault diagnosis framework. These two methods preserve the intrinsic advantages of LMD, such as robustness to outliers, distribution-free assumption, and high sensitivity for incipient faults. By analyzing the relative position between faulty samples and their corresponding anchors, the proposed fault isolation method can efficiently allow to recognize the single faulty variable even for tiny faults. Subsequently, thanks to a theoretical study, the fault severity estimation approach analytically establishes the relation between fault severity and the LMD index, offering an effective way to estimate the severity of incipient faults. In the CSTR case study, for incipient faults with FNR larger than 5 dB, the total accuracy of the proposed isolation method reaches 100%, and the relative error of the estimation method is less than 50%. The comparative study indicates that our approaches significantly outperform other typical methods for the incipient fault isolation and severity estimation tasks.

Despite the promising performance illustrated in this work, the LMD-based incipient fault diagnosis method should be improved in some aspects. First, the proposed isolation method is developed for single faulty source cases. Although its generalization to multiple faults cases has been discussed in this paper, reliability is usually hard to guarantee for complex situations. Accordingly, the LMD-based fault isolation method for multiple faults cases should be designed in future work. Secondly, the additive fault assumption and a first-order model are used to represent the fault's evolution, which is effective but less flexible. Therefore, a more general fault model for fitting complex evolution will be further investigated.

Acknowledgments

The authors would like to thank China Scholarship Council for funding.

References

[1] Alcala, C.F., Qin, S.J., 2009. Reconstruction-based contribution for process monitoring. Automatica 45, 1593–1600.

[2] Ashraf, S., Gao, M., Chen, Z., Naeem, H., Ahmad, A., Ahmed, T., 2020. Underwater pragmatic routing approach through packet reverberation mechanism. IEEE Access 8, 163091–163114.

[3] Basseville, M., 1989. Distance measures for signal processing and pattern recognition. Signal processing 18, 349–369.

[4] Canizo, M., Triguero, I., Conde, A., Onieva, E., 2019. Multi-head CNN–RNN for multi-time series anomaly detection: An industrial case study. Neurocomputing 363, 246–260.

[5] Chen, H., Jiang, B., Lu, N., 2017a. Data-driven incipient sensor fault estimation with application in inverter of high-speed railway. Mathematical Problems in Engineering 2017.

[6] Chen, Z., Cao, Y., Ding, S.X., Zhang, K., Koenings, T., Peng, T., Yang, C., Gui, W., 2019. A distributed canonical correlation analysis-based fault detection method for plant-wide process monitoring. IEEE Transactions on Industrial Informatics 15, 2710–2720.

[7] Chen, Z., Ding, S.X., Peng, T., Yang, C., Gui, W., 2017b. Fault detection for non-Gaussian processes using generalized canonical correlation analysis and randomized algorithms. IEEE Transactions on Industrial Electronics 65, 1559–1567.

[8] De Maesschalck, R., Jouan-Rimbaud, D., Massart, D.L., 2000. The Mahalanobis distance. Chemometrics and intelligent laboratory systems 50, 1–18.

[9] Delpha, C., Diallo, D., Al Samrout, H., Moubayed, N., 2018. Multiple incipient fault diagnosis in three-phase electrical systems using multivariate statistical signal processing. Engineering Applications of Artificial Intelligence 73, 68–79.

[10] Delpha, C., Diallo, D., Youssef, A., 2017. Kullback-Leibler divergence for fault estimation and isolation: Application to Gamma distributed data. Mechanical Systems and Signal Processing 93, 118–135.

[11] Harmouche, J., Delpha, C., Diallo, D., 2014. Incipient fault detection and diagnosis based on Kullback–Leibler divergence using principal component analysis: Part I. Signal processing 94, 278–287.

[12] Harmouche, J., Delpha, C., Diallo, D., 2015. Incipient fault detection and diagnosis based on Kullback–Leibler divergence using principal component analysis: Part II. Signal Processing 109, 334–344.

[13] Harmouche, J., Delpha, C., Diallo, D., 2016a. Incipient fault amplitude estimation using KL divergence with a probabilistic approach. Signal Processing 120, 1–7.

[14] Harmouche, J., Delpha, C., Diallo, D., Le Bihan, Y., 2016b. Statistical approach for nondestructive incipient crack detection and characterization using Kullback-Leibler divergence. IEEE Transactions on Reliability 65, 1360–1368.

[15] Isermann, R., 2005. Model-based fault-detection and diagnosis–status and applications. Annual Reviews in control 29, 71–85.

[16] Ji, H., 2021. Statistics Mahalanobis distance for incipient sensor fault detection and diagnosis. Chemical Engineering Science 230, 116233.

[17] Ji, H., He, X., Shang, J., Zhou, D., 2016. Incipient sensor fault diagnosis using moving window reconstruction-based contribution. Industrial & Engineering Chemistry Research 55, 2746–2759.

[18] Ji, H., He, X., Shang, J., Zhou, D., 2018. Exponential smoothing reconstruction approach for incipient fault isolation. Industrial & Engineering Chemistry Research 57, 6353–6363.

[19] Ji, H., Huang, K., Zhou, D., 2019. Incipient sensor fault isolation based on augmented Mahalanobis distance. Control Engineering Practice 86, 144–154.

[20] Jiang, Q., Yan, X., Huang, B., 2019. Review and perspectives of data-driven distributed monitoring for industrial plant-wide processes. Industrial & Engineering Chemistry Research 58, 12899–12912.

[21] Kroll, A., Schulte, H., 2014. Benchmark problems for nonlinear system identification and control using soft computing methods: Need and overview. Applied Soft Computing 25, 496–513.

[22] Li, X., Yang, X., Yang, Y., Bennett, I., Mba, D., 2019. A novel diagnostic and prognostic framework for incipient fault detection and remaining service life prediction with application to industrial rotating machines. Applied Soft Computing 82, 105564.

[23] Mansouri, M., Nounou, M.N., Nounou, H.N., 2017. Multiscale kernel PLS-based exponentially weighted-GLRT and its application to fault detection. IEEE Transactions on Emerging Topics in Computational Intelligence 3, 49–58.

[24] Pilario, K.E., 2021. Feedback-controlled CSTR process for fault simulation. https://www.mathworks.com/matlabcentral/fileexchange/66189-feedback-controlled-cstr-process-for-fault-simulation. Retrieved October 25, 2021.

[25] Pilario, K.E.S., Cao, Y., 2018. Canonical variate dissimilarity analysis for process incipient fault detection. IEEE Transactions on Industrial Informatics 14, 5308–5315.

[26] Safaeipour, H., Forouzanfar, M., Casavola, A., 2021. A survey and classification of incipient fault diagnosis approaches. Journal of Process Control 97, 1–16.

[27] Samuel, R.T., Cao, Y., 2015. Kernel canonical variate analysis for nonlinear dynamic process monitoring. IFAC-PapersOnLine 48, 605–610.

[28] Wang, B., Lei, Y., Li, N., Li, N., 2018. A hybrid prognostics approach for estimating remaining useful life of rolling element bearings. IEEE Transactions on Reliability 69, 401–412.

[29] Yang, J., Delpha, C., 2021a. A local Mahalanobis distance analysis based methodology for incipient fault diagnosis, in: 2021 IEEE International Conference on Prognostics and Health Management (ICPHM), IEEE. pp. 1–8.

[30] Yang, J., Delpha, C., 2021b. Local Mahalanobis Distance envelope using a robust healthy domain approximation for incipient fault diagnosis, in: IECON 2021 The 47th Annual Conference of the IEEE Industrial Electronics Society, IEEE. pp. 1–5.

[31] Yang, J., Delpha, C., 2022. An incipient fault diagnosis methodology using local Mahalanobis distance: Detection process based on empirical probability density estimation. Signal Processing 190, 108308.

[32] Yin, S., Ding, S.X., Haghani, A., Hao, H., Zhang, P., 2012. A comparison study of basic data-driven fault diagnosis and process monitoring methods on the benchmark Tennessee Eastman Process. Journal of process control 22, 1567–1581.

[33] Youssef, A., Delpha, C., Diallo, D., 2016. An optimal fault detection threshold for early detection using Kullback–Leibler divergence for unknown distribution data. Signal Processing 120, 266–279.

[34] Yu, J., Liu, X., Ye, L., 2021a. Convolutional long short-term memory autoencoder-based feature learning for fault detection in industrial processes. IEEE Transactions on Instrumentation and Measurement 70, 1–15.

[35] Yu, M., Lu, H., Wang, H., Xiao, C., Lan, D., Chen, J., 2021b. Computational intelligence-based prognosis for hybrid mechatronic system using improved wiener process, in: Actuators, Multidisciplinary Digital Publishing Institute. p. 213.

[36] Yue, H.H., Qin, S.J., 2001. Reconstruction-based fault identification using a combined index. Industrial & engineering chemistry research 40, 4403–4414.

[37] Zhang, J., Zhan, W., Ehsani, M., 2019. Fault-tolerant control of PMSM with inter-turn short-circuit fault. IEEE Transactions on Energy Conversion 34, 2267–2275.

[38] Zhang, K., Jiang, B., Yan, X.G., Mao, Z., 2017. Incipient voltage sensor fault isolation for rectifier in railway electrical traction systems. IEEE Transactions on Industrial Electronics 64, 6763–6774.

[39] Zhang, X., Delpha, C., Diallo, D., 2020a. Incipient fault detection and estimation based on Jensen–Shannon divergence in a data-driven approach. Signal Processing 169, 107410.

[40] Zhang, X., Delpha, C., Diallo, D., 2020b. Jensen-Shannon divergence for non-destructive incipient crack detection and estimation. IEEE Access 8, 116148–116162.

[41] Zhao, C., Gao, F., 2017. A sparse dissimilarity analysis algorithm for incipient fault isolation with no priori fault information. Control Engineering Practice 65, 70–82.